Electrohydrodynamic Gas Flow Regime Map in a Wire-Plate Type Electrostatic Precipitator

J. S. Chang and K. Urashima
Department of Engineering Physics, McMaster University, Canada

Abstract—It is well known that Electrohydrodynamically (EHD) induced secondary flow, i.e. so called ionic wind; normally reduce a particle collection efficiency of electrostatic precipitators (ESPs). However, the origin of this EHD secondary flow may now proposed to be initiated from the corona wire and grounded plate electrode separated. The flow pattern generated by EHD secondary form is more complex but categorized recently to 5 patterns as follows; 1. EHD wake flow; 2. EHD induced von Karman vortex stream; 3. Forward EHD wake; 4.Full EHD vortex downstream; and 5. Full Channel EHD vortex regimes. In this work, new combined parameter *Ehd*/Re^2 was introduced to simplified flow regime maps based on two parameters (*Ehd*/Re^2)$_{cw}$ based on corona wire and (*Ehd*/Re^2)$_{ch}$ based on flow channel, and EHD flow regime map was developed for the negative voltage ESP operations. The results show that the parameter *Ehd*/Re^2 is effective to predict EHD flow regime for various size and design of ESPs.s

Keywords—Electrostatic Precipitator, EHD Flow, Dust Particle Collection, Flow Regime Map

I. INTRODUCTION

The transport and precipitation of dust particles in ESPs depends on the particle properties, electric field, space charge and gas flow field. It was shown (e.g. [1, 2]) that a significant interaction between these factors exists, under main flow with EHD secondary flow included with EHD on-set of turbulence. However, there is not yet clear whether these EHD induced vortex and turbulent flow structures impact on the fine particle precipitation process, since the flow pattern map based on the dimensionless number for scaling was not well established on ESPs.

Recently the Particle Image Velocimetry (PIV) [3] based on the scattering of laser light on the particles following the flow was introduced for instantaneous measurement of the multi-dimensional flow velocity field, including the turbulence. In this work, new combined parameter *Ehd*/Re^2 was introduced to simplified flow regime maps based on two parameters (*Ehd*/Re^2)$_{cw}$ based on corona wire and (*Ehd*/Re^2)$_{ch}$ based on flow channel, and EHD flow regime map was developed for the both positive and negative voltage ESP operations based on recent published PIV and Schliren optical image observations and numerical simulations worldwide.

II. FLOW REGIME MAP

Dimensionless parameters used in the text were defined as follows:

$$\mathrm{Re} = \frac{LU_0}{\nu_g};\ Ehd = \frac{L^3 I_T}{\mu_i \rho_g {\nu_g}^2 A};\ Sc_d = \frac{\nu_g}{D_d};\ F_E = \frac{eV_0}{kT}$$

where Re is the Reynolds number, *Ehd* is the Electrohydrodynamic (EHD) number, *Sc* is the Schmidt number, F_E is the electric field number, L [m] is the characteristic length, U_0 [m/s] is the mean gas velocity, ν_g [m^2/s] is the gas kinematic viscosity, I_T [A] is the total discharge current, A [m^2] is surface area of the collecting electrode, ρ_g [kg/m^3] is the gas density, μ_i [m^2/Vs] is the ion mobility, D_d is the dust diffusion coefficient, V_0 [V] is the applied voltage magnitude, T [K] is the gas temperature, k = 1.381 x 10^{-23} [J/K] is the Boltzmann constant, and e = 1.602 x 10^{-19} [C] is elementary charge.

Other parameters used in the text:

$\vec{u}_g$ is the dimensionless gas velocity vector, n_d is the dimensionless dust particle number density, and $\vec{\xi}$ is the dimensionless electric field vector.

Typical EHD induced flow pattern can be categorized for 4 patterns as summarized in Fig. 1 and defined as follows:

Pattern [A]. On-Set of EHD von Karman vortex stream - in a cylinder in cross flow, the on-set of steady wake behind cylinder is Re = 7 and the wave becomes unstable when Re > 80. So called von Karman vortex stream with multiple waves initiated after Re = 10^4. However, EHD induced von Karman vortex stream type pattern as shown in Fig. 1 [A] generated even low Reynolds number (Re << 100) but larger EHD numbers. EHD-VKVS (von Karman vortex stream) normally not growing as ordinary Pattern [B]. On-set of EHD forward wakes - a forward wake as similar to the MHD flow also can be generated in EHD flow, where the forward wake is defined as wake generated at upstream of cylinder.

Pattern [C]. Attachment of EHD wakes in downstream flow channel. EHD flow no longer considered as near wire phenomenon after this pattern.

Pattern [D]. Attachment of EHD wakes in upstream flow channel.

Typical numerical results [9] for different *Ehd* numbers at fixed Reynolds number at 11.84 are show in Fig. 2, where E0, E1, E2, E3, E4 and E5 corresponding

Corresponding author: Jen-shih Chang
e-mail address: changj@mcmaster.ca

Presented at the International Symposium on Electro-hydro-dynamics, in March 2009

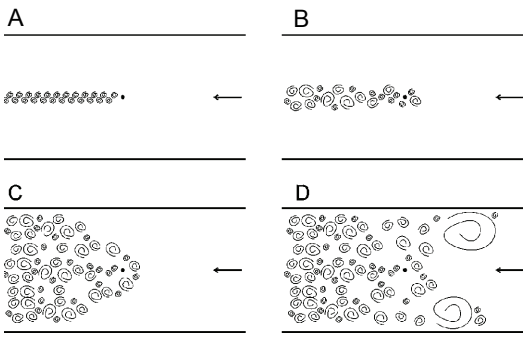

Fig. 1. EHD Flow structures with increasing applied voltage and current from (A) to (D).

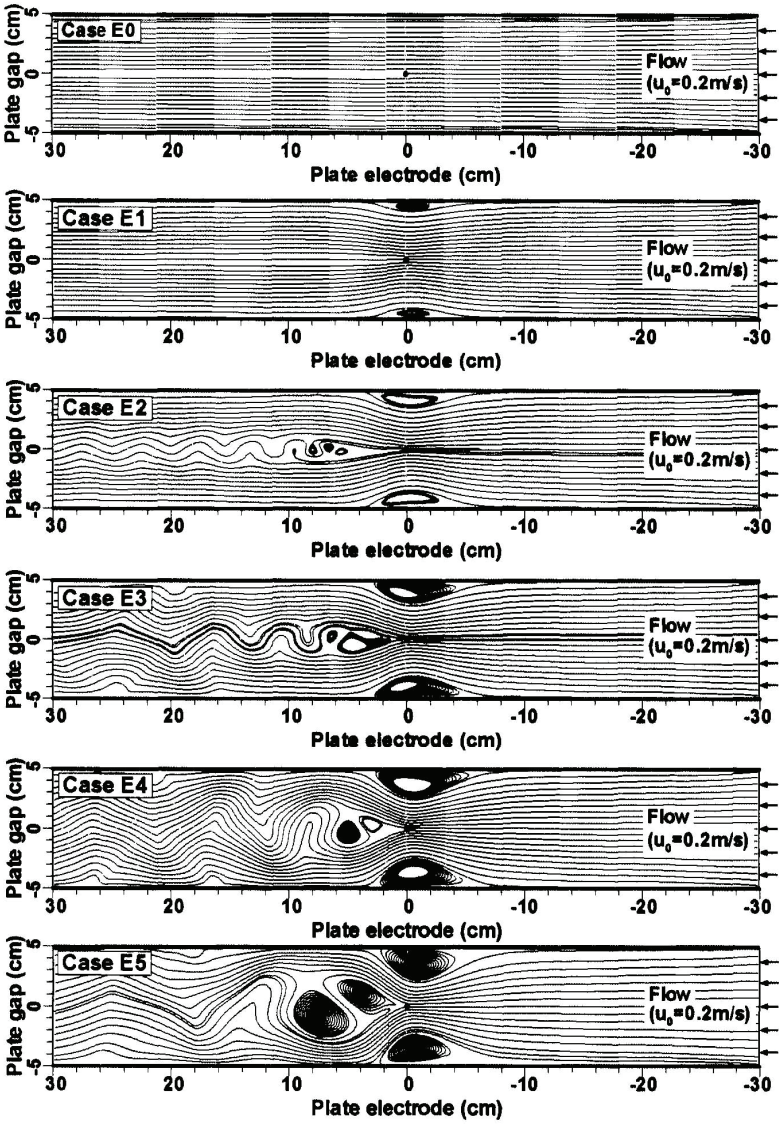

Fig. 2. Typical flow pattern transitions as a function of *Ehd* numbers for Re_{cw} = 1.2 [9], where E0, E1, E2, E3, E4 and E5 corresponding to Ehd_{cw} at 0, 388, 582, 776, 1164, 1746 respectively.

to Ehd_{cw} at 0, 388, 582, 776, 1164, 1746 respectively. Flow pattern of E1 is clearly type B but the other E2 to E5 are flow pattern D. All those flow patterns can be plotted against Reynolds number based on corona wire diameter Re_{cw} and based on flow channel width Re_{ch} with EHD number based on corona wire Ehd_{cw} and based on flow channel Ehd_{ch} as shown in Fig. 3, where the experimental results of Chang *et al.* [11] is shown as solid line and data points, the numerical modeling of Chun *et al.* [9] is shown by dashed lines, and the numerical results of Zhao and Adamiack [10] is shown by arrowed lines. Fig. 3 shows that the pattern [A] observed Re_{cw} (< 70) but smaller Ehd_{cw} (< 4 x 10^2) as expected as local near wire phenomenon.

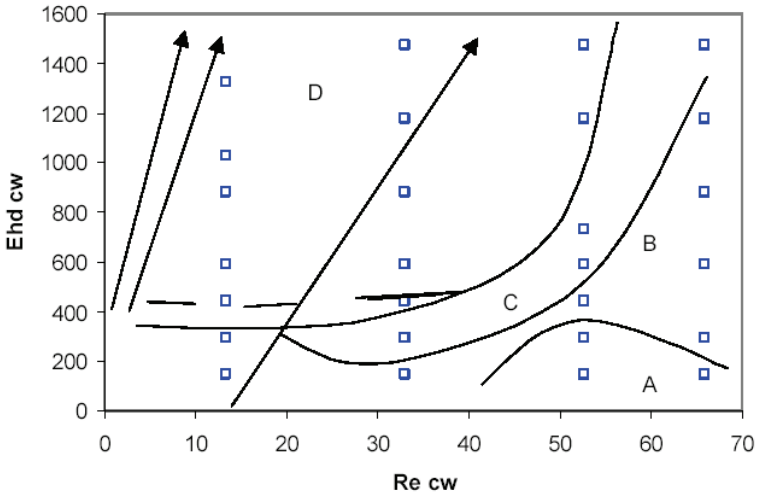

Fig. 3. Flow regime map under negative corona,
where solid line and data points: Chang *et al.* [11]; dashed lines: Chun *et al.* [9]; and arrowed lines: Zhao and Adamiack [10].

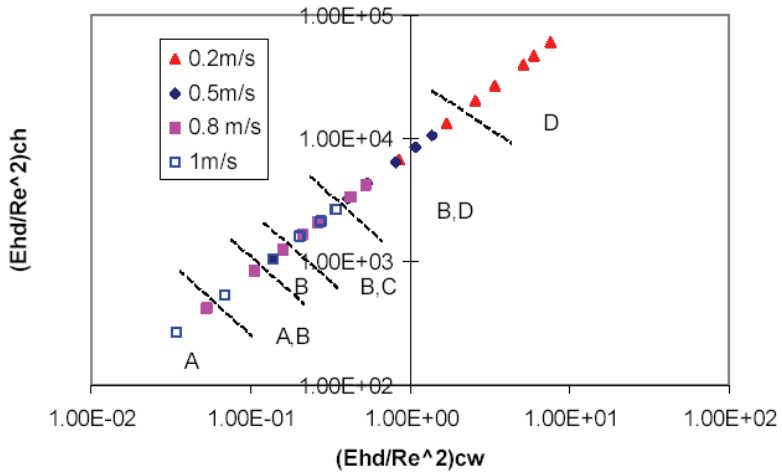

Fig. 4. Flow regime map based on Ehd/Re^2 based on corona wire and flow channel.

The transitions to pattern [A] to [B] occurs when $Ehd_{cw} > 4 \times 10^2$, however EHD wake immediately attach to the downstream channel wall when $\mathrm{Re}_{cw} < 50$ (Pattern [C]). Only larger Re_{cw} (> 50), main gas flow can maintain pattern [B] even at larger Ehd_{cw} (< 5 x 10^2) except numerical results of Zhao and Adamiack [10]. The numerical results of Chun *et al.* [9] are very close to the experimental results of Chang *et al.* [11]. The discrepancy between two models may be due to the different turbulent model used by Chun *et al.* and Zhao and Adamiack or may be due to the mismatching of discharge current used between two models.

The region covered by pattern [D] is wide and dominant when $(Ehd/\mathrm{Re}^2)_{ch} > 10$ as shown in Fig. 4, where $(Ehd/\mathrm{Re}^2)_{ch}$ as a function of $(Ehd/\mathrm{Re}^2)_{cw}$ for various flow pattern is shown. Figs. 3 and 4 shows that EHD flow becomes dominant near corona wire when $(Ehd/\mathrm{Re}^2)_{cw} > 1$ (Pattern A and B). The EHD flow becomes dominant near channel wall when $(Ehd/\mathrm{Re}^2)_{ch} > 2$ (Patterns C and D) as expected from the dimensional analyses of the momentum conservation equations by Chang and Watson [7].

III. Dust Particle Collection Efficiency

Transport of dust particles ($d_p < 1$ μm) can be expressed by the dimensionless particle transport equations [6, 7] as follows:

$$\frac{\mathrm{Re}_g\, Sc_d}{2}\vec{u}_g\tilde{\nabla}n_d \pm F_E\tilde{\nabla}(n_d\vec{\xi}) - \tilde{\nabla}^2 n_d = 0$$

Hence, EHD induced secondary flow become dominant effect when $\mathrm{Re}_g Sc_d/F_E < 1$ [8]. Based on the MESP code simulation [8, 12], the local particle charging for diameter between $0.1 < d_p < 1$ μm will be most significantly influenced by the EHD flow. Hence for flow patterns [A] and [B], the corona wire contamination occurs due to the EHD wake flow and the part of dusts

transported outside ESPs. However, for flow patterns [C] and [D], the dust particle collection may be enhanced due to EHD wakes attachment to the ESP collection electrode in flow channel wall. However, based on the recent numerical modeling [12], the overall and partial collection efficiencies for ESP will not influenced by EHD flow.

IV. Concluding remarks

In this paper, the flow velocity fields flow regime map in the wire-plate type ESP were developed for a wide range of Reynolds and EHD numbers based on published experimental and numerical works. The results showed a four typical EHD induced flow patterns in the ESP as follows: (A) EHD induced von Karman vortex stream; (B) on-set of forward EHD wake; (C) Attachment of EHD wake in downstream; and (D) Attachment of EHD forward wake in upstream. In order to obtain scaling of EHD flow phenomena, flow pattern map was presented. The relatively good agreement between modeling and experiments are obtained. The results also show that the parameter Ehd/Re^2 is effective to predict EHD flow regime for various size and design of ESPs.

Acknowledgment

Authors thank J. Mizeraczyk, M. Kocik, J. Podinski, L. Zho, K. Adamiack, D. Brocilo, A. A. Berezin, G. Touchard, H. Fujishima and T. Yamamoto for various discussions and comments. This work is supported by NSERC of Canada.

References

[1] T. Yamamoto and H. R. Velkoff, "Electrodynamics in an Electrostatic Precipitator," *J. Fluid Mech.*, vol.108, pp. 1-16, 1981.

[2] W. J. Liang and T. H. Lin, "The Characteristics of Ionic Wind and its Effect on Electrostatic Precipitators," *Aerosol Sci. Technol.*, vol. 20, pp. 330-337, 1994.

[3] J. Westerweel, "Fundamentals of Digital Particle Image Velocimetry," *Meas. Sci. Technol.*, vol. 8, pp.1379-1388, 1997.

[4] J. Mizeraczyk, M. Kocik, J. Dekowski, M. Dors, J. Podliński, T. Ohkubo, S. Kanazawa, and T. Kawasaki, "Measurement of the Velocity Field of the Flue Gas Flow in an Electrostatic Precipitator Model using PIV method," *J. Electrostatics*, vol. 51-52, pp. 272-278, 2001.

[5] J. Mizeraczyk, J. Dekowski, J. Podliński, M. Kocik, T. Ohkubo, and S. Kanazawa, "Laser Flow Visualization and Velocity Fields by Particle Image Velocimetry in an Electrostatic Precipitator Model," *J. Visualization*, vol. 6, no. 2, pp. 125-133, 2003.

[6] IEEE-DEIS-EHD Technical Committee, *IEEE Trans. Dielectrics and Electrical Insulation*, vol. 10, no. 1, pp. 3-6, 2003.

[7] J. S. Chang and A. Watson, "Electromagnetic Hydrodynamics," *IEEE Trans. Dielectrics and Electrical Insulation*, vol. 5, no.1, pp. 871-895,1994.

[8] J. S. Chang, "Next Generation Integrated Electrostatic Gas Cleaning System," *J. Electrostatics*, vol. 57, pp. 273-219, 2003.

[9] Y. N. Chun, A. A. Berezin, J. S. Chang, and J. Mizeraczyk, "Numerical Modeling of Near Corona Wire Electrohydrodynamic Flow in a Wire-plate Electrostatic Precipitator," *IEEE Trans. Dielectrics and Electrical Insulation*, vol. 14, no.1, pp. 119-124, 2007.

[10] L. Zho and K. Adamiack, "Numerical Simulation of the Electrohydrodynamic Flow in a Single Wire-Plate Electrostatic Precipitator," *IEEE Trans. Industry Applications*, vol. 44, no. 2, pp. 683-691, 2008.

[11] J. S. Chang, J. Dekowski, J. Podliński, D. Brocilo, K. Urashima, and J. Mizeraczyk, "Electrohydrodynamic Gas Flow Regime Map in a Wire- Plate Electrostatic Precipitator," in *IEEE Industry Applications Society 2005 Annual Meeting*, in CD, 2005.

[12] D. Borocilo, A. A. Berezin, and J.S. Chang, *Proc. ISESP X*, pp. 129-133, 2008.

[13] H. Fujishima, Y. Morita, M. Okubo, and T. Yamamoto, "Numerical Simulation of Three-dimensional Electrohydrodynamics of Spite-Electrode Electrostatic Precipitators," *IEEE Trans. Dielectrics and Electrical Insulation*, vol. 13, pp. 160-167, 2006.

[14] T. Yamamoto, M. Okuda, and M. Okubo, "Three–dimension Ionic Winds and Electrohydrodynamics of Tuft/Point Corona Electrostatic Precipitator," *IEEE Trans. Industry Applications*, vol. 39, no. 6, pp. 1602-1607, 2003.

[15] S. J. Park and S.S. Kim, "Effect of Electrohydrodynamic Flow and Turbulent Diffusion on Collection Efficency of Electrostatic Precipitator with Cavity Walls," *Aerosol Sci. & Technology*, vol. 37, no. 7, pp. 574-586, 2003.